# crystallization communications

# Crystallization and preliminary X-ray analysis of *Aspergillus oryzae* catechol oxidase

**Heidi Kaljunen,[a] Chiara
Gasparetti,[b] Kristiina Kruus,[b]
Juha Rouvinen[a] and Nina
Hakulinen[a]***

[a]Department of Chemistry, University of Eastern
Finland, Joensuu Campus, PO Box 111,
FIN-80101 Joensuu, Finland, and [b]VTT
Technical Research Center of Finland,
PO Box 1000, FIN-02044 VTT, Finland

Correspondence e-mail: nina.hakulinen@uef.fi

Catechol oxidase is an enzyme that catalyzes the oxidation of *o*-diphenols to the corresponding *o*-quinones. It is a copper-containing enzyme with a binuclear copper active site. Here, the crystallization and multiple-wavelength anomalous dispersion data collection of catechol oxidase from the mould fungus *Aspergillus oryzae* are described. During the purification, three forms of the enzyme (39.3, 40.5 and 44.3 kDa) were obtained. A mixture of these three forms was initially crystallized and gave crystals that diffracted to 2.5 Å resolution and belonged to space group $P3_221$, with unit-cell parameters $a = b = 118.9$, $c = 84.5$ Å, $\alpha = \beta = 90$, $\gamma = 120°$. A preparation containing only the shorter form (39.3 kDa) produced crystals that diffracted to 2.9 Å resolution and belonged to space group $P2_12_12_1$, with unit-cell parameters $a = 51.8$, $b = 95.3$, $c = 139.5$ Å, $\alpha = \beta = \gamma = 90°$.

## 1. Introduction

Catechol oxidase (EC 1.10.3.1) is one of the type 3 copper proteins, which also include tyrosinase and the oxygen-carrier protein haemocyanin. Catechol oxidase and tyrosinase are strongly related since they both catalyze the oxidation of *o*-diphenols to the corresponding quinones. In addition to this, tyrosinases are also able to orthohydroxylate monophenols to diphenols (monophenol monooxygenase; EC 1.14.18.1). In the catecholase reaction electrons are transferred from the diphenol substrate to molecular oxygen, resulting in reduction of the dioxygen to water and formation of the quinone product. Quinones are highly reactive species and can autopolymerize to form a brown polyphenolic pigment called melanin (Rompel *et al.*, 1999). Catechol oxidases are mainly found in plant tissues, where the formation of quinone polymerization products is thought to protect the damaged tissue from pathogens and insects (Eicken *et al.*, 1999; Gerdemann *et al.*, 2002; Marusek *et al.*, 2006).

Although catechol oxidases (also referred to in the literature as polyphenol oxidases or PPOs) have been isolated and purified from a wide variety of plants and fruits (Gerdemann *et al.*, 2002), only two crystal structures of this enzyme are available at present. These are the three-dimensional structure of the 39 kDa isoform of the *Ipomoea batatas* (sweet potato) catechol oxidase (PDB entry 1bt1; Klabunde *et al.*, 1998) and the very recently solved three-dimensional structure of the enzyme from the grape *Vitis vinifera* (PDB code 2p3x; Virador *et al.*, 2010). In these structures the dicopper centre is surrounded by a four-helix bundle, which is also observed in the known tyrosinase structure from *Streptomyces castaneoglobisporus* (Matoba *et al.*, 2006) and in known haemocyanin structures (Volbeda & Hol, 1998; Hazes *et al.*, 1993; Cuff *et al.*, 1998; Perbandt *et al.*, 2003). All six histidines coordinating the two coppers are located in this four-helix bundle.

Spectroscopic and structural information from tyrosinases and catechol oxidases and also from haemocyanins has been used to unravel the mechanism behind the enzyme activities of both tyrosinase and catechol oxidase. Based on the information available, several mechanisms for both the monophenolase and the diphenolase activities of tyrosinase and catechol oxidase have been proposed (Solomon *et al.*, 1996; Eicken *et al.*, 1999; Koval *et al.*, 2006). These
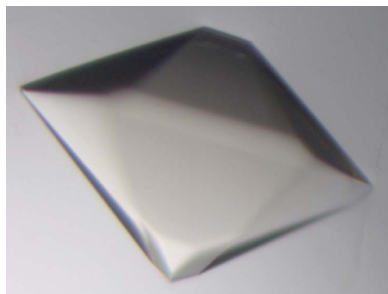
mechanisms differ from each other in some aspects and without additional structural information the precise mechanisms of the two type 3 copper enzymes remain unclear together with the question of the substrate specificity of tyrosinases and catechol oxidases.

Here, we describe the crystallization and preliminary crystallographic analysis of a fungal catechol oxidase from *Aspergillus oryzae*. Based on amino-acid sequence, *A. oryzae* catechol oxidase shows only weak identity (<20%) to plant catechol oxidases and a bacterial tyrosinase. The structural characterization may provide useful information for elucidating the mechanism of binuclear copper enzymes.

## 2. Materials and methods

### 2.1. Expression and purification

The isolation of the catechol oxidase gene from *A. oryzae*, its expression in *Trichoderma reesei* and the purification process of the enzyme have been described by Gasparetti *et al.* (2010). This fungal enzyme was originally considered to belong to the class of short tyrosinases, but was later classified as a catechol oxidase based on its enzymatic activity. Initially, crystallization experiments were carried out using a preparation containing three forms of the enzyme with molecular masses of approximately 39.3, 40.5 and 44.3 kDa. Later, a more homogeneous preparation was obtained from pool 1 containing only the 39.3 kDa form of the *A. oryzae* catechol oxidase. The crystallization and preliminary X-ray studies of both enzyme preparations are described in this article.

### 2.2. Crystallization

Crystallization experiments were performed using the hanging-drop vapour-diffusion method in Linbro 24-well plates (Hampton Research). For initial screening of the original enzyme preparation, the commercial crystallization kits Clear Strategy Screens I and II (Molecular Dimensions) were used and crystallization was carried out at room temperature. In the initial crystallization experiments, 1 µl protein solution at a concentration of 5 mg ml$^{-1}$ and 1 µl crystallization solution were equilibrated against 500 µl reservoir solution which consisted of 450 µl stock solution and 50 µl Tris pH 7.5 buffer from the crystallization kit. Small crystals appeared during 24 h and grew in a drop that contained 1.8 *M* lithium sulfate solution (Clear Strategy Screen II solution No. 8). During optimization, the droplet size was increased to 4 µl containing equal amounts of protein solution and crystallization solution. *A. oryzae* catechol oxidase crystallized with various buffers in the pH range 4.5–9.0. Two visually different crystal forms were found, one growing in the pH range 4.5–

6.0 and the other in the pH range 7.0–9.0 (Figs. 1*a* and 1*b*). Although the space groups of the two crystal forms were the same, the unit-cell size was larger for the crystal that grew in the alkaline pH range. The best crystals were obtained when a slightly lower precipitant concentration (1.7 *M*), ammonium sulfate instead of lithium sulfate and sodium acetate buffer pH 4.5 were used. Adding a small amount of glycerol to the crystallization solution greatly improved the resistance of the crystals to handling but at the same time decreased the size of the crystals. We also discovered that for both crystal forms the crystal colour changed first from colourless to green and eventually turned to brown during storage.

For crystallization experiments on the pool 1 enzyme preparation, two commercial screens (Crystal Screen from Hampton Research and Clear Strategy Screen from Molecular Dimensions) were used in the initial screening. Small needle-like crystals were obtained from three different crystallization conditions that contained either 0.2 *M* lithium sulfate, 0.2 *M* magnesium chloride or 0.3 *M* sodium acetate in addition to 10% polyethylene glycol (PEG) 8000 and 10% PEG 1000 and Tris pH 7.5 buffer. Several optimization screens were carried out and the best measurable crystals grew in a solution that consisted of 12% PEG 8000, 10% ethanol, 0.2 *M* magnesium chloride and 0.1 *M* sodium acetate buffer pH 4.5 (Fig. 1*c*). Optimization of these crystals is still in progress.

### 2.3. X-ray data collection and processing

X-ray data were collected from crystals of the original enzyme preparation on beamline X12 at the DESY synchrotron in Hamburg. This is a tuneable beamline with an energy range from 5.5 to 18 keV (2.1–0.7 Å) and is equipped with a 225 mm MAR Mosaic CCD detector. Prior to data collection, the crystals were soaked in cryoprotectant solution containing 25% glycerol and were stored in liquid nitrogen. A total of four data sets were collected: MAD data at three different wavelengths and a high-resolution data set at a wavelength of 1.0 Å. Prior to the MAD data collection, an X-ray fluorescence spectrum for copper was measured using a Bruker/AXS PX-XFlash energy-sensitive X-ray fluorescence detector. Based on this spectrum, suitable wavelengths for MAD data collection were chosen. Three data sets were collected: one at the Cu *K* absorption edge at a wavelength of 1.37633 Å (9.008 keV; peak), one at a wavelength of 1.37756 Å (9.000 keV; inflection) and the last at a wavelength of 1.37497 Å (9.017 keV; remote). Each data set, including the high-resolution set, consisted of a minimum of 90 images and was collected using a 1° oscillation angle. Recently, we also collected X-ray data from tiny crystals of the pool 1 enzyme preparation on beamline ID29 at the ESRF synchrotron in Grenoble. 25% glycerol was again used
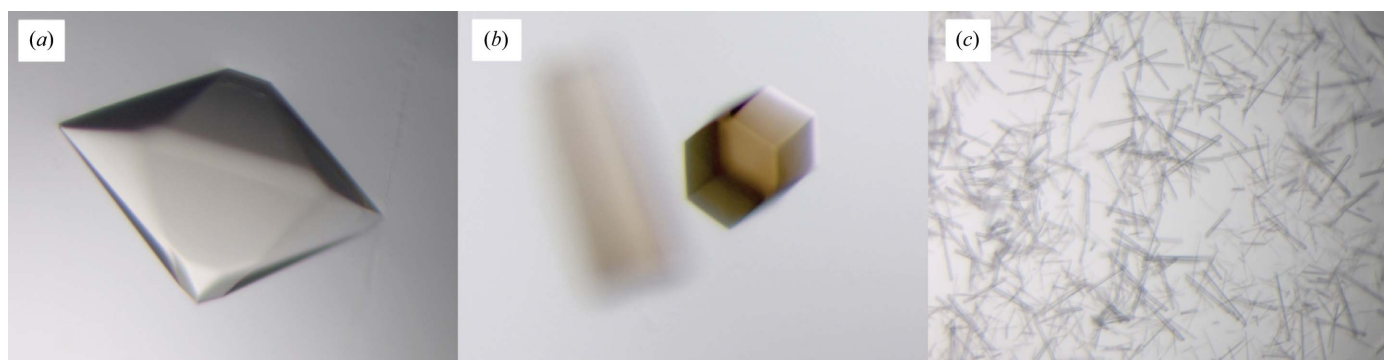


**Figure 1**
Crystals of *A. oryzae* catechol oxidase. (*a*) A crystal growing in solution consisting of 1.7 *M* ammonium sulfate, 5% glycerol and 0.1 *M* sodium acetate pH 4.5. (*b*) A crystal growing in solution consisting of 1.7 *M* lithium sulfate and 0.1 *M* Tris–HCl buffer pH 8.0. (*c*) Needle-like crystals from pool 1 of the *A. oryzae* catechol oxidase.

**Table 1**
Data-collection and processing statistics for *A. oryzae* catechol oxidase crystals.

Values in parentheses are for the highest resolution shell.

|  | Peak | Inflection | Remote | High resolution | Pool 1 |
|---|---|---|---|---|---|
| Wavelength (Å) | 1.37633 | 1.37756 | 1.37497 | 1.0 | 0.9724 |
| No. of images | 80 | 100 | 90 | 90 | 180 |
| Oscillation (°) | 1 | 1 | 1 | 1 | 0.5 |
| Resolution (Å) | 2.8 (2.9–2.8) | 2.8 (2.9–2.8) | 3.1 (3.2–3.1) | 2.5 (2.6–2.5) | 2.9 (3.0–2.9) |
| Observed reflections | 83678 (8281) | 104438 (10163) | 62383 (5660) | 119367 (13574) | 55618 (5417) |
| Unique reflections | 32753 (3263) | 32441 (3249) | 23324 (2166) | 43241 (4918) | 14921 (1447) |
| Completeness (%) | 98.2 (99.2) | 97.3 (98.9) | 94.8 (97.2) | 93.5 (95.8) | 93.6 (95.8) |
| $R_{merge}$† (%) | 4.5 (37.8) | 4.1 (30.6) | 4.4 (27.9) | 5.1 (28.8) | 11.6 (43.1) |
| $\langle I/\sigma(I)\rangle$ | 16.5 (2.5) | 20.5 (3.2) | 19.5 (4.0) | 15.6 (4.4) | 14.4 (5.5) |

† $R_{merge} = \sum_{hkl} \sum_i |I_i(hkl) - \langle I(hkl)\rangle| / \sum_{hkl} \sum_i I_i(hkl)$.

as a cryoprotectant and 180 images with 0.5° oscillation angle were collected. Data processing was carried out for all data sets using the program *XDS* and scaling was performed using *XSCALE* (Kabsch, 2010).

## 3. Results and discussion

The originally used preparation contained three forms of *A. oryzae* catechol oxidase with molecular masses of 39.3, 40.5 and 44.3 kDa and produced measurable crystals from various different conditions. A MAD data set and a high-resolution data set were collected from crystals that grew in solution consisting of 1.7 *M* ammonium sulfate and 0.1 *M* sodium acetate buffer pH 4.5. The crystals diffracted to 2.5 Å resolution and belonged to space group $P3_221$, with unit-cell parameters $a = b = 118.9$, $c = 84.5$ Å, $\alpha = \beta = 90$, $\gamma = 120°$. The solvent content was calculated with the Matthews formula (Matthews, 1968) using a molecular mass of 40.5 kDa. This gave a $V_M$ of 2.1 Å$^3$ Da$^{-1}$ and a solvent content of 42% assuming the presence of two molecules in the asymmetric unit, or a $V_M$ of 4.3 Å$^3$ Da$^{-1}$ and a solvent content of 71% assuming the presence of one molecule in the asymmetric unit. A crystal from the pool 1 enzyme preparation containing only the shorter enzyme form (39.3 kDa) grew in solution consisting of 12% PEG 8000, 10% ethanol, 0.2 *M* magnesium chloride and 0.1 *M* sodium acetate buffer pH 4.5. This crystal diffracted to 2.9 Å resolution and belonged to space group $P2_12_12_1$, with unit-cell parameters $a = 51.8$, $b = 95.3$, $c = 139.5$ Å, $\alpha = \beta = \gamma = 90°$. Calculation of the Matthews coefficient suggested the presence of two molecules in the asymmetric unit ($V_M = 2.2$ Å$^3$ Da$^{-1}$) with a solvent content of 44%. Data-collection and processing statistics are presented in Table 1.

We initially used the multiwavelength anomalous dispersion (MAD) method to calculate the phases of the protein using the program *SHELXC/D/E* (Sheldrick, 2008). Although the locations of the Cu atoms could be determined and electron-density maps were calculated, the phasing power of the coppers was not sufficient to produce interpretable electron-density maps for the whole protein molecule. For this reason, a combination of the single-wavelength anomalous dispersion (SAD) and molecular-replacement methods with the additional information of the known copper positions was used. The structure of the *S. castaneoglobisporus* tyrosinase was used as a molecular model since this enzyme has the highest sequence identity (19%) to the studied *A. oryzae* catechol oxidase. The MR

solution clearly contained one protein molecule in the asymmetric unit and automated model building with the program *Buccaneer* from *CCP*4 (Winn *et al.*, 2011) managed to build four helices around the coppers but failed to build the model further. However, the resultant electron-density map was clearly interpretable and refinement of the model is currently in progress.

## References

Cuff, M. E., Miller, K. I., van Holde, K. E. & Hendrickson, W. A. (1998). *J. Mol. Biol.* **278**, 855–870.
Eicken, C., Krebs, B. & Sacchettini, J. C. (1999). *Curr. Opin. Struct. Biol.* **9**, 677–683.
Gasparetti, C., Faccio, G., Arvas, M., Buchert, J., Saloheimo, M. & Kruus, K. (2010). *Appl. Microbiol. Biotechnol.* **86**, 213–226.
Gerdemann, C., Eicken, C. & Krebs, B. (2002). *Acc. Chem. Res.* **35**, 183–191.
Hazes, B., Magnus, K. A., Bonaventura, C., Bonaventura, J., Dauter, Z., Kalk, K. H. & Hol, W. G. (1993). *Protein Sci.* **2**, 597–619.
Kabsch, W. (2010). *Acta Cryst.* D**66**, 125–132.
Klabunde, T., Eicken, C., Sacchettini, J. C. & Krebs, B. (1998). *Nature Struct. Biol.* **5**, 1084–1090.
Koval, I. A., Gamez, P., Belle, C., Selmeczi, K. & Reedijk, J. (2006). *Chem. Soc. Rev.* **35**, 814–840.
Marusek, C. M., Trobaugh, N. M., Flurkey, W. H. & Inlow, J. K. (2006). *J. Inorg. Biochem.* **100**, 108–123.
Matoba, Y., Kumagai, T., Yamamoto, A., Yoshitsu, H. & Sugiyama, M. (2006). *J. Biol. Chem.* **281**, 8981–8990.
Matthews, B. W. (1968). *J. Mol. Biol.* **33**, 491–497.
Perbandt, M., Guthöhrlein, E. W., Rypniewski, W., Idakieva, K., Stoeva, S., Voelter, W., Genov, N. & Betzel, C. (2003). *Biochemistry*, **42**, 6341–6346.
Rompel, A., Fischer, H., Meiwes, D., Büldt-Karentzopoulos, K., Magrini, A., Eicken, C., Gerdemann, C. & Krebs, B. (1999). *FEBS J.* **445**, 103–110.
Sheldrick, G. M. (2008). *Acta Cryst.* A**64**, 112–122.
Solomon, E. I., Sundaram, U. M. & Machonkin, T. E. (1996). *Chem. Rev.* **96**, 2563–2606.
Virador, V. M., Reyes Grajeda, J. P., Blanco-Labra, A., Mendiola-Olaya, E., Smith, G. M., Moreno, A. & Whitaker, J. R. (2010). *J. Agric. Food Chem.* **58**, 1189–1201.
Volbeda, A. & Hol, W. G. (1998). *J. Mol. Biol.* **209**, 249–279.
Winn, M. D. *et al.* (2011). *Acta Cryst.* D**67**, 235–242.